Assembly and Dissociation of Human Insulin and $Lys^{B28}Pro^{B29}$-Insulin Hexamers: A Comparison Study

Duane T. Birnbaum,[1] Maureen A. Kilcomons,[1] Michael R. DeFelippis,[1] and John M. Beals,[2,3]

Received August 14, 1996; accepted November 1, 1996

Purpose. Investigations into the kinetic assembly and dissociation of hexameric $Lys^{B28}Pro^{B29}$-human insulin (LysPro), a rapid-acting insulin analog produced by the sequence inversion of amino acids at positions B28 and B29, were designed to explain the impact that the sequence inversion has on the formulation and pharmacokinetics of the insulin analog.

Methods. The kinetics of phenolic ligand binding to human insulin and LysPro were studied by stopped-flow spectroscopy. The kinetics of R_6 hexamer disruption were studied by extraction of Co(II) with EDTA.

Results. Phenolic ligand binding to human insulin yielded rate constants for a fast and slow phase that increased with increasing ligand concentration and are attributed to the $T_6 \rightarrow T_3R_3$ and $T_3R_3 \rightarrow R_6$ transitions, respectively. However, the kinetics of phenolic ligand binding with LysPro was dominated by rates of hexamer assembly. The kinetic differences between the insulin species are attributed to alterations at the monomer-monomer interface in the dimer subunit of the LysPro analog. The extraction of Co(II) from both hexameric complexes by EDTA chelation is slow at pH 8.0 and highly dependent on ligand concentration. Cobalt extraction from LysPro was pH dependent. Of the various phenolic ligands tested, the relative affinities for binding to the human and LysPro hexamer are resorcinol > phenol > m-cresol.

Conclusions. The extraction data support the formation of an R_6-type LysPro hexamer under formulation conditions, i.e., in the presence of divalent metal and phenolic ligand, that is similar in nature to that observed in insulin. However, the formation kinetics of LysPro identify a radically different monomeric assembly process that may help explain the more rapid pharmacokinetics observed with the hexameric formulation of LysPro insulin relative to human insulin.

KEY WORDS: $Lys^{B28}Pro^{B29}$-human insulin; insulin; cobalt insulin hexamers; hexameric association; hexameric dissociation.

INTRODUCTION

Commercial insulin preparations contain phenolic excipients (e.g., phenol, m-cresol, and methylparaben) as antimicrobial agents. These phenolic species also bind to specific sites on the insulin hexamers, In_6M_2 (M = Zn(II), Co(II)), causing a conformational change that increases the chemical stability of insulin (1). X-ray crystallographic studies identified the location of six binding sites on the insulin hexamer and the nature of the conformational change that the binding of these phenolic ligands induces (2). In addition, spectroscopic (3) and crystallographic (2,4,5) data on Zn(II)-insulin and Co(II)-insulin hexamers in the presence and absence of phenolic excipients have identified three distinct hexameric species: T_6, T_3R_3,[4] and R_6, where T_3R_3 is an intermediate structure with the liganded insulin molecules of one trimer in an R-state conformation and the unliganded insulin molecules in the other trimer in a T-state conformation. Thus, it has been proposed that the insulin hexamer behaves as a dimer of trimers, and the binding process is represented by the following equilibria: $T_6 \leftrightarrow T_3R_3 \leftrightarrow R_6$ (7).

Solution studies on Zn(II)- and/or Co(II)-insulin have qualitatively identified the presence of positive and negative homotropic cooperativity during the binding of these ligands (7–9). In Co(II)-insulin hexamers, the intra-trimer ligand binding is thought to be modulated by positive cooperativity and the inter-trimer ligand binding modulated by negative cooperativity (9).

Previous reports have included kinetic measurements for both R_6 hexamer formation and disruption (10–13). Kinetic measurements of the $T \rightarrow R$ structural transition in Co(II)-insulin induced by phenol or m-cresol revealed a biphasic reaction (12). The observed rate for the fast phase ($T_6 \rightarrow T_3R_3$) was first order with respect to the ligand, whereas the observed rate for the slow phase ($T_3R_3 \rightarrow R_6$) was reported to remain independent of ligand concentration. The authors did not attempt to model the ligand concentration-dependent rates, thus n^{th} order rate constants were not reported. Regarding Zn(II)-insulin, detailed kinetic measurements for the disruption of the T_6 and T_3R_3 hexamers were obtained by using tridentate metal ion chelators under varying concentrations and Zn(II)/insulin ratios (10,11); however, only preliminary, extraction studies on the R_6 state have been reported (10).

$Lys^{B28}Pro^{B29}$-human insulin (LysPro[5]) is a modified human insulin in which the amino acids Lys^{B29} and Pro^{B28} have been inverted. LysPro was designed to be monomeric and consequently faster-acting providing the user more convenience and improved glucose control after meals. Relative to human insulin, the association of LysPro monomers into hexamers is hindered due to a reduced dimerization constant (approximately 300-fold) (14). This dramatic reduction in the self-association characteristics of the analog relative to human insulin is illustrated in Scheme 1. Despite this tremendous decrease in the dimer self-association, in the presence of metal ions and phenolic ligands (15), X-ray crystallography has revealed the presence of both $T_3R_3^f$ (6) and R_6-type LysPro hexamers (16). The structure of the $T_3R_3^f$ hexamer is similar to that of human insulin, with the same stoichiometry and binding sites for the metal ions and phenolic ligands. The identification of a $T_3R_3^f$ LysPro structure from X-ray crystallography, and the biphasic nature of ITC and CD binding profiles (15) suggest that negative inter-trimer cooperativity still plays a role in the binding of phenolic

[1] Division of Biopharmaceutical Development, Lilly Research Laboratories, Eli Lilly and Company, Indianapolis, Indiana 46285.

[2] Eli Lilly and Company, Lilly Research Laboratories, Lilly Corporate Center, Drop Code 3848, Indianapolis, Indiana 46285.

[3] To whom correspondence should be addressed.

ABBREVIATIONS: $Lys^{B28}Pro^{B29}$-human insulin (LysPro); isothermal titrating calorimetry (ITC); circular dichroism (CD); molecular weight cut-off (MWCO); optical density (OD); phenolic ligand (ϕ); ethylenediaminetetraacetic acid (EDTA).

[4] Recently, a detailed review of all X-ray crystallographic results concerning the human-insulin hexamer intermediate structure has resulted in the reclassification of the hexamer as $T_3R_3^f$, where only residues B4-B19 are α-helical (6). However, far UV-CD data still supports the presence of a T_3R_3 hexamer in solution.

[5] LysPro, Humalog™, is an approved pharmaceutical for the treatment of diabetes.

0724-8741/97/0100-0025$12.50/0

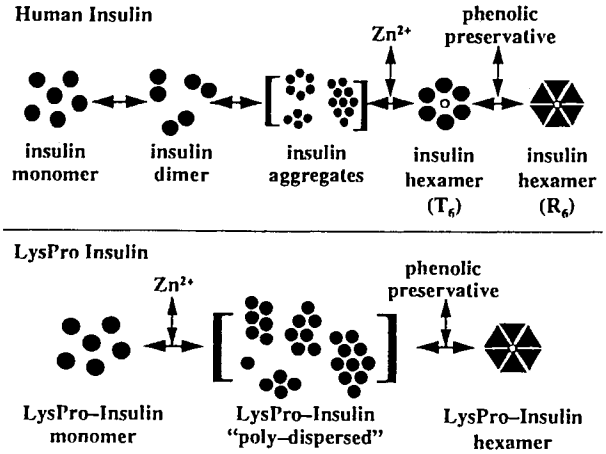

Scheme 1. Human- and $Lys^{B28}Pro^{B29}$-insulin association. The self-association properties of (top) insulin and (bottom) LysPro-insulin. Insulin readily associates into dimers and higher-order aggregates that, in the presence of M(II) (e.g., Zn(II) or Co(II)), associate into discrete T_6 hexameric complexes. These T_6 hexamers can be converted to R_6 hexamers by the binding of phenolic ligands, e.g., phenol or m-cresol, that are routinely used as antimicrobial agents in insulin formulations. In contrast, LysPro-insulin can only form discrete hexameric complexes in the presence of M(II) (e.g., Zn(II) or Co(II)) and phenolic ligands. This is presumably due to the weakened dimerization constant (~300-fold) of LysPro-insulin.

ligands. Interestingly, the ability of LysPro to self-associate in discrete hexamers increases the chemical stability of the molecule (15) and thus provides a means for a viable pharmaceutical formulation. However, minimal kinetic information on hexameric formation and disruption has been generated to help explain the retention of fast-action despite hexameric complexation (17).

Based on the association/dissociation properties of insulin, a pharmacokinetic model for soluble insulin formulations proposed by Brange *et al.* (18) describes a series of events occurring upon subcutaneous injection of soluble insulin formulations (Scheme 1). The initial step in their model involves the dissociation of phenolic preservative from the hexameric complex converting the formulated R_6 hexamer to the T_6 hexamer. The T_6 hexamer then dissociates into monomers after a 10^5 reduction in insulin concentration (10^{-3} M → 10^{-8} M) via diffusion from the subcutaneous site. This diffusion process delays the pharmacokinetics of current soluble formulations of human insulin. Clinical studies on LysPro insulin have demonstrated more rapid absorption into the circulatory system from a subcutaneous injection (17). A pharmacokinetic model proposed by Ciszak *et al.* (6) for pharmaceutically formulated LysPro insulin involves the direct dissociation of the Zn(II) $Lys^{B28}Pro^{B29}$-insulin hexameric complex to monomeric insulin (Scheme 1) after the diffusion of phenolic preservative occurs at the subcutaneous site, due in part, to the loss of a critical hydrophobic interaction at the monomer-monomer interface of the dimer subunit. Consequently, LysPro can dissociate without a concomitant dilution of the protein.

Thus, to further understand the association and dissociation properties of the LysPro hexameric complex, and the relationship to physiological activity and pharmacokinetics, we have explored the kinetics of its assembly and disruption under various solution conditions. It was necessary to use Co(II) rather than Zn(II) so the reaction could be monitored spectroscopically. The absorption maximum of the R_6 Co(II)-insulin complex is red-shifted from the T_6 complex by 85 nm with an increase in ϵ_{max} of more than one order of magnitude (8). Zn(II) is optically transparent (UV-VIS) in both octahedral and tetrahedral coordination geometries.

MATERIALS AND METHODS

Sample Preparation

Human and LysPro insulins were produced by recombinant DNA techniques at Eli Lilly and Company and supplied as Zn(II) crystals. The proteins were dissolved in water, treated with Chelex 100 resin (Bio-Rad) to remove any metal, filtered, and dialyzed (Spectra/Por*7 regenerated cellulose dialysis membrane; nominal MWCO 2000) against four liters of ultrapure water (Milli-Q Plus water purification system, Millipore Co.) for approximately six hours at room temperature. Insulin and LysPro concentrations were determined from their absorption at 276 nm, ϵ_{276} = 6100 M^{-1} cm^{-1} (14,19). Final solutions contained 50 mM Tris/Cl^- at pH 7.1 or 8.0 and insulin concentrations of 10 and 6 mg/mL for the extraction and formation kinetic experiments, respectively. A volume of Co(II) (as the chloride) solution was added to achieve a 1:3 stoichiometric ratio with insulin monomer, i.e., 1 mole of cobalt per 3 moles of insulin monomer. The phenolic ligand concentration was varied in the range 0 to 80 mM. Protein solutions (before the addition of phenolic ligand) were passed through sterile 0.2-μm filters prior to use. Liquefied distilled phenol (89%) and distilled m-cresol were obtained from Eli Lilly and Company and were of the highest pharmaceutical grade. Resorcinol was obtained from Aldrich Chemical Company and purified by sublimation.

Kinetics

Extraction studies used sample volumes of 1 mL in a 1-cm pathlength cell. A 10-μL aliquot of a 0.5 M EDTA solution was quickly added and manually mixed with a Teflon paddle just prior to data collection (dead time approximately 10 seconds). The absorbance decay profiles at 580 nm representing the kinetic time course for metal ion extraction were measured on an AVIV 14DS UV-visible spectrophotometer.

Formation kinetics were measured on a Bio-Logic SFM3 stopped-flow module equipped with three injection syringes that contained stock solutions of insulin, ligand and buffer. The volume of insulin stock injected into the cell was held constant while the ligand, and buffer volumes were varied such that the total volume injected into a 1-cm pathlength cell was 400 μL. Absorbance changes were monitored at 580 nm. The theoretical dead time for mixing was 35 milliseconds.

For both formation and extraction experiments, the ligand concentration was kept in large excess of hexamer concentration assuring pseudo-first-order conditions. Each time course was measured three to five times and averaged. Data generated over a ligand concentration range was also repeated three to five times.

Ultracentrifugation

Sedimentation velocity data was measured using a Beckman Model E analytical ultracentrifuge with Schlieren optics and a double sector 12-mm pathlength cell running at 60,000 rpm at 22°C for 135 minutes. A total of 15 photographs were taken at 8-minute intervals. Five photographs taken in the middle of the experiments were used for analysis. Sedimentation coefficients were calculated for LysPro solutions (1.0 mM in LysPro, 0.33 mM Co(II), 50 mM Tris/Cl^- at pH 7.1 and 8.0) using the method described by van Holde (20). Phenol concentrations were varied between 0 and 50 mM.

Sedimentation equilibrium experiments were done under the same conditions in the absence of phenol using a Beckman Optima XLA analytical ultracentrifuge. The sedimentation data was collected at a rotor speed of 8000 rpm, an absorbance wavelength of 251 nm (O.D. minimum), and a cell pathlength of 3 mm. System equilibration occurred after approximately 24 hours.

Treatment of the Kinetic Data

Both formation and extraction time courses were fit with mono- and bi-exponential functions using standard linear least-squares techniques. The following equation represents the five-parameter bi-exponential function used to fit the data.

$$Absorbance = Amp_{\text{fast}} \times exp(-k_{\text{fast}} \times t) + Amp_{\text{slow}} \times exp(-k_{\text{slow}} \times t) + y_{\text{asy}} \quad (1)$$

Amp_{fast} and Amp_{slow} *are the amplitudes corresponding to the fast and slow phase with observed rates* k_{fast}[6] and k_{slow}. The absorbance asymptote is given by y_{asy}, and t is the time. Eliminating one exponential term results in the three-parameter function used to fit the mono-exponential time courses.

Mechanism for Phenolic Ligand Binding

The mechanism used to interpret the data generated by phenolic ligand binding to Co(II) insulin hexamers is influenced by the literature, where it is widely believed that the crystallographically identified T_6, T_3R_3, and R_6 hexamers are the dominant species present in solution (7–10,12,21,22). Furthermore, these species exist in a dynamic equilibrium that heavily favors the T_6 hexamer in the absence of phenolic ligands and high concentrations of anions, but shifts to the R_6 hexamer as phenolic ligands are introduced into solution. The hexamer can be represented as a dimer of trimers with the binding of phenolic ligands modulated by intra- and inter-trimer cooperativity. Assuming the following equilibrium,

$$T_6 + 3\phi \underset{k_{-1}}{\overset{k_1}{\rightleftarrows}} T_3R_3 \quad (2)$$

$$T_3R_3 + 3\phi \underset{k_{-2}}{\overset{k_2}{\rightleftarrows}} R_6 \quad (3)$$

where the phenolic ligand concentration, $[\phi]$, is in large excess of the insulin hexamer concentration, k_1 and k_2 are the rate constants for association, in $M\ s^{-1}$, for ligand binding to the first and second trimer, k_{-1} and k_{-2} are the rate constants for dissociation, in s^{-1}, for ligand dissociation to the first and second trimer. Under the concentration employed in this study, the rates for k_1 and k_2 are fast relative to k_{-1} and k_{-2}. Thus, the rate law for each phase is pseudo-first-order, and has the form:

$$\frac{d[hexamer]}{dt} = k_x[hexamer][\phi]^y \quad (4)$$

The ligand concentration is essentially constant; therefore, the n^{th}-order rate constants ($n = y + 1$) for each phase of the reaction are given by k_x ($x = 1$ or 2). The concentration of T_3R_3 or R_6 species is given by $[hexamer]$. This leads to a ligand-concentration dependence on the observed rates for the fast phase,

$$k_{fast} = k_1[\phi]^{y1} \quad (5)$$

and for the slow phase,

$$k_{slow} = k_2[\phi]^{y2} \quad (6)$$

Using these equations to fit plots of the observed rate (k_{fast} or k_{slow}) versus ligand concentration allows for the determination of the n^{th}-order rate constants k_1 and k_2.

Intra-trimer cooperativity, and the possibility of competing rates of binding pocket formation, will decrease the effect that ligand concentration has on the observed rate. Therefore, the expected cubic-power dependence of the ligand concentration is replaced by an adjustable parameter (y) when fitting the data. The value of this parameter will be referred to as the apparent number of ligand binding sites per trimer. We could also choose a function that represented the observed rate as a sum of two different kinetic processes, both including a ligand-concentration dependence with different but integer-power dependencies (e.g., $k_{slow} = k_2[\phi]^2 + k_3[\phi]^3$). Although such an equation would provide an equally good fit with the same number of adjustable parameters as equation 6, it is inconsistent with the trimer-wise binding mechanism proposed here and in the literature as correct for insulin/phenolic ligand solutions. Therefore, we model our data with the simpler but more consistent equations (5 and 6).

Mechanism for Co(II) Extraction

In the R_6 human-insulin hexamer, the metal ions are buried deep within the molecule such that accessibility to the solvent is highly restricted (2). Therefore, we assume that metal ion extraction will only occur via more accessible T/R intermediates, e.g., T_3R_3. Thus, the R_6 hexamer is the only state from which metal cannot be extracted. A simple mechanistic path can be written as follows,

$$R_6 \underset{k_2}{\overset{k_{-2}}{\rightleftarrows}} T_yR_{6-y} + y\phi + Cl^- \quad (7)$$

and

$$T_yR_{6-y} + EDTA \xrightarrow{k} \text{Products} \quad (8)$$

where k includes all mechanistic steps following the formation of the EDTA-hexamer complex, and is assumed to be fast

[6] It should be noted that k_{slow}, k_{fast}, and k_{obs} refer to kinetic rates and that k_1, k_2, k_{-1}, k_{-2}, and k refer to rate constants throughout the text.

relative to k_{-2}, which is rate-limiting. Chloride anion is included in this equation since it occupies the fourth ligand position in the tetrahedrally-coordinated metal; however, the formation of the intermediate T_yR_{6-y} presumably leads to a non-tetrahedrally coordinated metal that is coordinated to water. The octahedrally coordinated metal in the T_3 state is liganded to 3 water molecules and three histidine residues. Thus, the rate law is given by

$$rate = k[EDTA][T_yR_{6-y}] \quad (9)$$

which becomes

$$rate = \frac{kk_{-2}[EDTA][R_6]}{k[EDTA] + k_2[\phi]^y[Cl^-]} \quad (10)$$

if the concentration of T_yR_{6-y} is assumed to reach a steady state; i.e., the *rate* is equal to $k_{obs} \cdot [R_6]$. Thus, the inverse of the observed reaction rate can be written as

$$\frac{1}{k_{obs}} = \frac{1}{k_{-2}} + \frac{k_2[Cl^-][\phi]^y}{kk_{-2}[EDTA]} \quad (11)$$

which allows for the easy extraction of k_{-2} from the intercept of $1/k_{obs}$ versus $[\phi]^y$. Once again, y is an adjustable parameter used to account for cooperativity. It should be emphasized that R_6 is the species being monitored and that the steady state production of T_yR_{6-y} is rapidly depleted by EDTA extraction of the Co(II) that destabilizes the hexamer. Consequently, exponential loss in R_6 is observed over the time course of the experiment.

RESULTS

Kinetic Profiles

Examples of time courses generated by phenolic ligand binding to, and Co(II) extraction from, the insulin hexamer are shown in Figure 1. The absorbance increase associated with R_3 formation around each metal site at the sub-saturating amount of ligand added is greatest for resorcinol followed by phenol and m-cresol (Figure 1A). The absorbance decrease upon Co(II) extraction with EDTA is much slower for resorcinol relative to phenol and m-cresol (Figure 1B). The three profiles representing R_6 formation are biphasic, whereas the three representing Co(II) extraction are monophasic.

Formation of T_3R_3 and R_6 Hexamers of Co(II)-Insulin

The dependence of the observed rates (fast and slow) for T_3R_3 and R_6 Co(II)-insulin hexamer formation on phenol concentration and their corresponding amplitudes are displayed in Figure 2. Both fast and slow rates have a strong, *nonlinear* dependence on phenol concentration; however, the power dependence (y) is greater for the slow phase (Table I). Similar behavior is observed with m-cresol and resorcinol. The nonlinear dependency of the observed rates on ligand concentration, and the convergence of relative amplitudes for the fast and slow phases to 0.5, were observed in Co(II)-insulin hexamers regardless of the ligand, pH, temperature, and insulin concentration studied. The magnitudes of the observed rates (k_{fast} and k_{slow}) are similar with each ligand and is minimally influenced by pH (tested 7.3 to 8.5) and insulin concentration. Lowering the temperature to 10°C decreases the rates by about one order of magnitude, but the nonlinear dependence on ligand concentration is maintained. Also shown in Figure 2 (A and B) is the fit to the simple kinetic model described earlier (eqns. 5 and 6). Values for the nth-order rate constants for the formation of T_3R_3 and R_6 insulin hexamers extracted from this model are given in Table I.

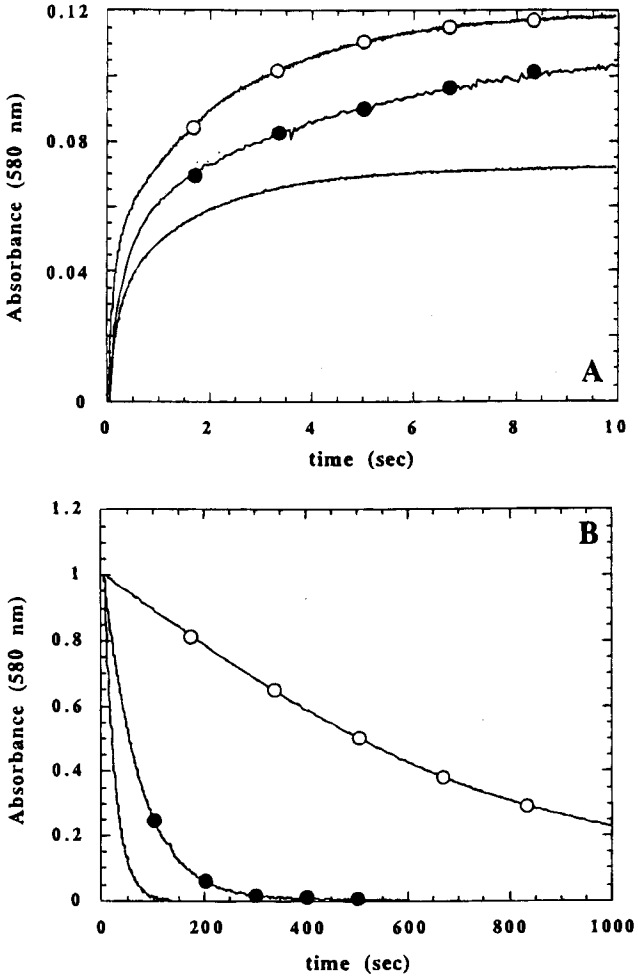

Fig. 1. Kinetic time courses for formation of, and metal ion extraction from, Co(II)-R_6-insulin hexamers. (A) Biphasic kinetic profile for ligand binding to Co(II)-insulin. These biphasic plots are fit to equation 1 to obtain k_{fast} and k_{slow}. Values obtained for k_{fast} and k_{slow} as a function of the ligand concentration are used to model ligand binding to the insulin hexamer. Conditions were 0.17 mM In_6Co_2, 50 mM Tris/Cl^-, pH = 8.0, and 25°C. (B) Monophasic kinetic profiles for metal ion extraction from Co(II)-insulin. Values of k_{obs} as a function of ligand concentration are used to model the extraction of Co(II) from insulin and LysPro insulin R_6 hexamers. For clarity, each kinetic profile generated by the extraction of Co(II) from the insulin hexamer has been normalized to its maximum intensity. Final conditions were 0.30 mM In_6Co_2, 5 mM EDTA, 50 mM Tris/Cl^-, pH = 8.0, and 25°C. Solutions were mixed manually with a dead time of ~10 seconds. Phenolic ligand concentration: (○) 25 mM resorcinol, (●) 25 mM phenol, (—) 25 mM m-cresol.

Formation of Hexameric Co(II)-LysPro

The binding of phenolic ligands to the Co(II)-LysPro hexamer yields kinetic profiles that are, at a minimum, biphasic

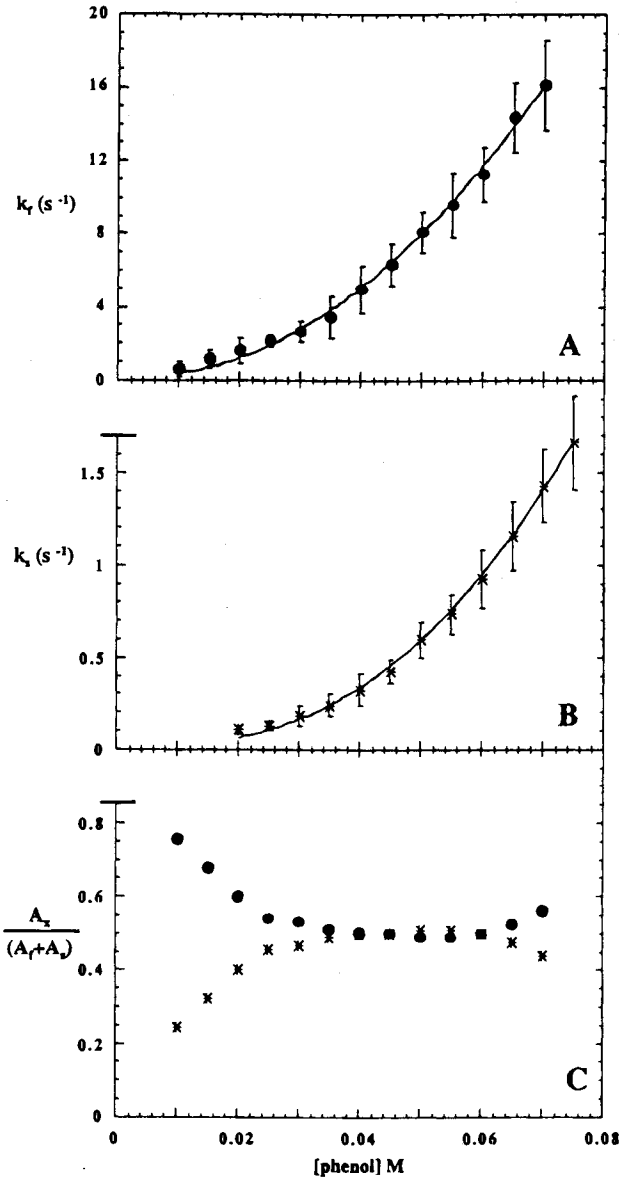

Fig. 2. Phenol concentration dependence on the observed rates and amplitudes of Co(II)-R_6-insulin hexamer formation. Ligand concentration dependence for phenol on (A) the rates of binding to Co(II)-insulin associated with the fast phase (●), (B) the rates of binding to Co(II)-insulin associated with the slow phase (*), and (C) the relative amplitudes of the two phases. Each point in the curve represents a rate constant extracted from fitting equation 1 to a time course (e.g., Figure 1) measured at the given ligand concentration. The subscripts f and s refer to the fast and slow phases, respectively. The subscript x in the y-axis label of (C) refers to either the fast or slow phase depending on which relative amplitude is calculated. The solid lines in (A) and (B) represent the best fit to the experimental data with equations 4 and 5 using standard linear least-squares techniques. Conditions were 0.17 mM In_6Co_2, 50 mM Tris/Cl^-, pH = 8.0, and 25°C.

(data not shown). At pH 8.0, the rates observed for both phases with phenol binding to the Co(II)-LysPro hexamer are independent of phenol concentration (Table II). Comparable binding rates (k_{obs}) are obtained for resorcinol with its value (averaged over the ligand concentration range used) given in Table II. The relative amplitudes of each phase are somewhat variable, but remain between 0.4 and 0.6.

For LysPro solutions at pH 8.0 and pre-treated with subsaturating concentrations of phenolic ligand (5 and 3 mM for phenol and resorcinol, respectively), the reaction remains biphasic. However, the ligand-concentration dependence on the fast rate becomes large and nonlinear. The slow rate remains at approximately the same constant value as with the data obtained from untreated samples (Figure 3, Table II). From equilibrium binding studies (data not shown), the addition of this small amount of phenolic ligand induces the formation of tetrahedral Co(II) centers producing a nearly identical optical absorption spectrum to that of R_6 Co(II)-insulin. The initial absorbencies of the pre-treated LysPro solutions are approximately 40% and 60% (phenol and resorcinol, respectively) of the absorbance measured when the hexamer is saturated with ligand. The fast phase dominates the amplitude, even more so with increasing affinity of the ligand (80% and 100% for phenol and resorcinol, respectively). The data are summarized in Table I using equation 5 to model the fast phase of the reaction.[7] Phenol and resorcinol bind to the LysPro hexamer with similar rates. Due to the decreased binding affinity and solubility of m-cresol, it was not possible to generate reliable data covering a sufficient ligand-concentration range. Therefore, the case of m-cresol binding of LysPro insulin will not be considered here.

With LysPro solutions containing Co(II), the kinetics of phenolic ligand binding are pH dependent. If the initial LysPro solution is not pre-treated with phenolic ligand, and the pH is lowered to 7.1, a fast rate is observed that is nonlinearly dependent on ligand concentration and of similar magnitude to the fast rate observed for ligand binding to the human insulin hexamer (Figures 2A and 4A). Modeling the phenol concentration dependence on the fast rate with equation 5, yields an n^{th}-order rate constant of $3.6 \times 10^4\ s^{-1}M^{-3}$, about a factor of two less than that at pH 8.0 with the LysPro solution pre-treated to 5 mM in phenol (Table I). At both pH 8.0 and 7.1, the ligand-concentration-power dependence for the fast rate is at or near 3.0, and the ligand-concentration-independent slow rate remains constant (Figure 4). In general, the n^{th}-order rate constants differ significantly between human and LysPro insulin (Table I).

Sedimentation Velocity and Equilibrium

The sedimentation coefficients measured for LysPro in the presence of Co(II) at pH 7.1 and 8.0 with various levels of phenol are given in Table III. At saturating levels of phenol (20 and 50 mM, respectively), the sedimentation coefficients are comparable to those of human insulin in the presence of Zn(II) and phenolic ligands, which is known to exist as a hexamer in solution (15). At pH 7.1 and 8.0, the Schlieren profiles for LysPro are symmetrical in the presence of saturating amounts of phenol. Similar sedimentation coefficients were measured for Co(II)-LysPro solutions in the presence of 5 mM phenol; however, the Schlieren profiles also indicate the presence of species smaller than hexamers, more so at pH 8.0 than

[7] By using eqn. 4, we are not making any assumptions about the existence of the equilibria given in eqn. (2) for the Co(II)-LysPro complex. Rather we are using a simple empirical relationship to fit what is clearly a nonlinear data set.

Table I. Modeling the Binding of Phenolic Ligands to, and Co(II) Extraction from, the Human- and LysPro-insulin Hexamers at 25°C

		Formation				Extraction			
Protein	Ligand pH	k_1 (s^{-1} M^{-y1})	y_1 (# of sites in trimer 1)	k_2 (s^{-1} M^{-y2})	y_2 (# of sites in trimer 2)	k_{-2} (s^{-1})	y ([Ligand] power dep.)	$K^{(kinetic)}$ (M^{-1})	$K^{(ITC)}$ (M^{-1})
human insulin	m-cresol pH 8.0	12000 (27)	2.2 (4)	14000 (31)	2.8 (4)	n.d.	n.d.	n.d.	n.d.
human insulin	phenol pH 8.0	5700 (19)	2.2 (3)	1900 (29)	2.7 (4)	0.028 (5)	1.8 (4)	6.8×10^4	7.5×10^4
human insulin	resorcinol pH 8.0	2800 (16)	1.6 (3)	2700 (28)	2.3 (4)	0.005 (18)	1.9 (6)	5.4×10^5	5.6×10^6
LysPro	phenol pH 8.0	n.d.	n.d.	8.8×10^4 (29)	2.8 (4)	0.093 (35)	3.1 (1)	4.9×10^7	n.d.
LysPro	phenol pH 7.1	n.d.	n.d.	3.6×10^4 (19)	3.0 (2)	0.093 (23)	1.1 (4)	n.d.	n.d.
LysPro	resorcinol pH 8.0	n.d.	n.d.	8.8×10^4 (19)	2.5 (2)	0.016 (60)	3.2 (2)	2.2×10^9	n.d.

Note: Values obtained from the fits to stopped-flow kinetic binding data using equations 1–5 in the text. With respect to LysPro insulin, only binding data that demonstrated a ligand-concentration dependence was modeled (fast phase at pH 7.1 and fast phase at pH 8.0 when pre-treated). The ligand concentration power dependence is given as the parameter y. It should be noted that only one ligand-concentration dependent phase was observed with LysPro and has arbitrarily been placed in k_2 and y_2 (see, explanation in text under section *pH 8.0 (pre-treated)*). Extraction data was modeled using equations 6–11. The equilibrium constant, $K^{(kinetic)}$ is the ratio of ligand on and off rate constants, i.e., k_2/k_{-2}, for the $T_3R_3 \leftrightarrow R_6$ equilibrium; however, it should be noted that for LysPro insulin that $K^{(kinetic)}$ is a K_{app}, i.e., $k_2/(k \cdot k_{-2})$, since k_2 cannot be accurately determined. K_{app} is the slope of the line derived from equation 11. The equilibrium constant, $K^{(ITC)}$, refers to the $T_3R_3 \leftrightarrow R_6$ equilibrium, with values obtained by modeling profiles generated by isothermal titration calorimetry (28,29). The term n.d. refers to not determined. The standard errors are reported in parentheses as percent of value.

pH 7.1 (data not shown). In the absence of phenol, the Schlieren profiles and coefficients indicate a polydisperse system with species ranging from monomer to high molecular weight aggregates at pH 7.1, and from monomer to relatively low-molecular-weight aggregates at pH 8.0.

Sedimentation equilibrium data measured for phenol-free Co(II)-LysPro solutions at 1.0 mM LysPro (concentration at which stopped-flow kinetic experiments were measured) gave weight-average molecular weights 7 and 23 times the monomer molecular weight at pH 8.0 and pH 7.1, respectively. The considerably higher molecular weights obtained at pH 7.1 relative to pH 8.0 are consistent with the sedimentation velocity experiments.

Table II. Experimental Rate Constants for Ligand Binding to LysPro Insulin

	pH 8.0 (untreated)		pH 8.0 (pre-treated)	pH 7.1 (pre-treated)
Ligand	$\overline{k_{fast}}$ (s^{-1})	$\overline{k_{slow}}$ (s^{-1})	$\overline{k_{slow}}$ (s^{-1})	$\overline{k_{slow}}$ (s^{-1})
m-cresol	n.d.	n.d.	0.05 (20)	n.d.
%S.E.				
phenol	0.21 (30)	0.04 (25)	0.06 (50)	0.13 (23)
%S.E.				
resorcinol	0.15 (13)	0.017 (18)	n.d.	n.d.
%S.E.				

Note: Observed rates are independent of ligand concentration and the reported values have been averaged over the ligand concentration range studied. Untreated refers to a solution that was initially free of phenolic ligand. The term n.d. refers to not determined. The standard errors are reported in parentheses as percent of value.

Extraction of Co(II) from R_6 Insulin and LysPro Hexamers

The monophasic extraction rates of Co(II) from R_6 insulin and R_6 LysPro hexamers and their dependence on phenol concentration at pH 8.0 are illustrated in Figure 5. The reaction is quite slow (minutes to hours) and the dependence of the observed rate on phenol concentration is nonlinear for both insulin and LysPro hexamers but to a greater degree for the latter. Comparable behavior is observed when resorcinol is the binding ligand (data not shown); however, the rates are slower (approximately a factor of 25). The data were fit to equation 11 and results are reported in Table I. Due to problems associated with insulin precipitation upon extraction when m-cresol was the phenolic ligand, a detailed concentration dependence with this ligand could not be measured. If initial conditions are such that a sub-saturating amount of ligand is present in solution, then the reaction will follow biphasic kinetics. With phenol, >95% of the binding sites are saturated at approximately 40 mM in insulin and approximately 20 mM in LysPro hexamers. When an extraction was carried out with a ligand concentration less than saturation, the slow rate extracted from the fit to the time course was used in the analysis.

It was determined that the concentration of EDTA had no effect on the observed extraction rate from R_6 insulin and LysPro hexamers and that all Co(II) was sequestered if EDTA was added in at least a 1:1 stoichiometric amount. Chloride concentration (50 mM, the minimum level required to ensure that the

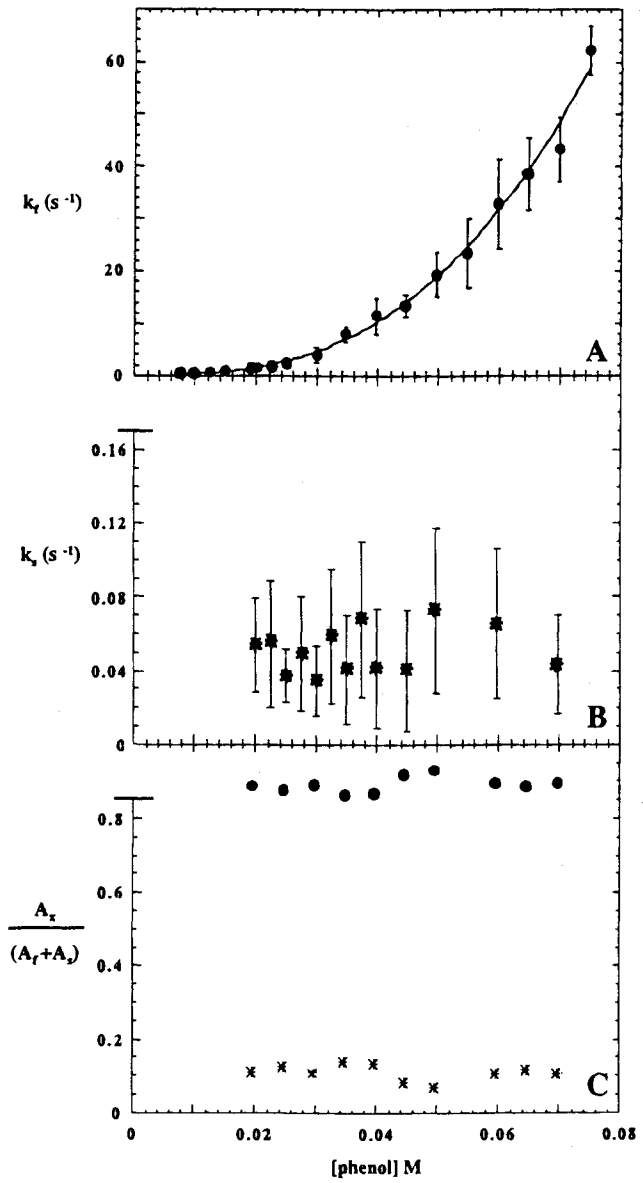

Fig. 3. Phenol concentration dependence on the observed rates and amplitudes of Co(II)-R_6-LysPro insulin hexamer formation at pH 8.0. Ligand concentration dependence for phenol on (A) the rates of binding to Co(II)-LysPro associated with the fast phase (●), (B) the rates of binding to Co(II)-insulin associated with the slow phase (*), and (C) the relative amplitudes of the two phases. Each point in the curve represents a rate constant extracted from fitting equation 1 to a time course (e.g., Figure 1) measured at the given ligand concentration. The subscripts f and s refer to the fast and slow phases, respectively. The subscript x in the y-axis label of (C) refers to either the fast or slow phase depending on which relative amplitude is calculated. The solid line in (A) represents the best fit to the experimental data with equation 4 using standard linear least-squares techniques. Final conditions were 0.17 mM In_6Co_2, 50 mM Tris/Cl^-, pH = 8.0, and 25°C. The initial LysPro insulin solution was pre-treated to 5 mM phenol.

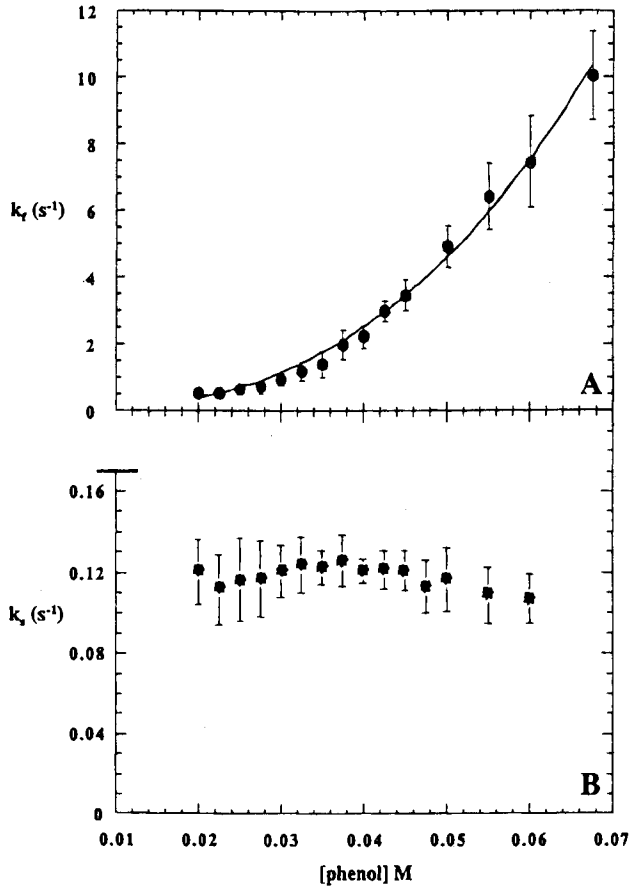

Fig. 4. Phenol concentration dependence on the observed rates of Co(II)-R_6-LysPro insulin hexamer formation at pH 7.1. Ligand concentration dependence for phenol on (A) the rates of binding associated with the fast phase (●) and (B) the rates of binding associated with the slow phase (*) in untreated Co(II)-LysPro solutions at pH = 7.1. The subscripts f and s refer to the fast and slow phases, respectively. Final conditions were 0.17 mM In_6Co_2, 50 mM Tris/Cl^-, pH = 7.1, and 25°C.

4^{th} binding site to Co(II) was Cl^- rather than the anion of a phenolic molecule) has an inverse linear relationship with the Co(II) extraction rate. Higher concentrations of chloride were avoided in order to maintain reasonable insulin solubility after the metal was extracted. The pH dependence was negligible

Table III. Sedimentation Coefficients for LysPro Insulin in the Presence of Co(II) at 23°C

	Sedimentation Coefficient, S	
[phenol] mM	pH = 7.1	pH = 8.0
0	6.6[c]	3.8[d]
5	3.5[b]	3.2[b]
20	3.4[a]	3.2[a]
50	3.4[a]	3.1[a]

Note: Qualitative descriptions are based on the relative homogeneity of the observed sedimentation profiles as well as results from sedimentation equilibrium experiments. Solutions were 0.17 mM In_6Co_2, 50 mM Tris/Cl^-. Errors are approximately ±10%.

[a] Symmetrical profile, primarily hexamer.

[b] Skewed symmetrical profile, predominantly hexamer with small population of lower MW species.

[c] Polydisperse, high MW aggregates (>100 kDa).

[d] Polydisperse, low MW aggregates (<45 kDa).

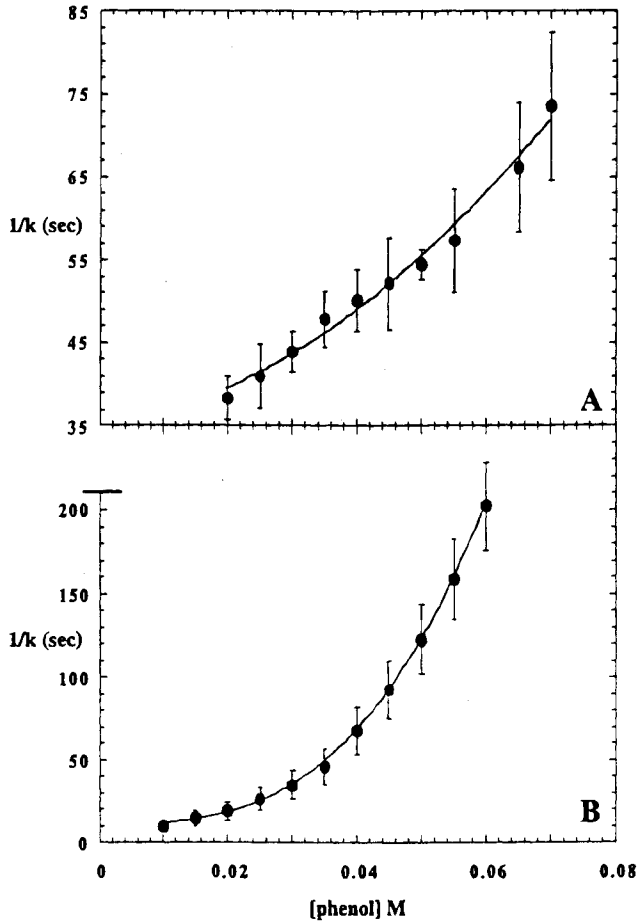

Fig. 5. Phenol concentration dependence on the observed rate of metal ion extraction from Co(II)-R_6 hexamers of insulin and LysPro insulin. Ligand-concentration dependence on the rate of extracting Co(II) from R_6 hexamers of (A) insulin and (B) LysPro insulin. Initial conditions were 0.30 mM In_6Co_2, 50 mM Tris/Cl^-, pH = 8.0, and 25°C.

between 7.3 and 8.5 for the extraction of Co(II) from R_6 insulin hexamers in the presence of a saturating amount of phenol. With LysPro hexamers, the extraction at pH 7.1 resulted in the same value for k_{-2} as at pH 8.0; however, the phenol concentration dependence on the observed rate was relatively minor (Table I).

Equilibrium Binding of Phenol to Co(II)-LysPro Insulin at pH 7.1 and 8.0

Visible absorption spectra measured for Co(II)-LysPro insulin solutions in the presence of saturating levels of phenol at pH 7.1 and 8.0 are nearly identical to spectra measured for the Co(II)-human insulin hexamer (data not shown). The titration of phenol into a Co(II)-LysPro solution yields simple monophasic binding profiles as monitored by the increasing absorbance of tetrahedral Co(II) centers. Greater than 95% of the binding sites are saturated at 20–25 mM phenol for 1.0 mM LysPro solutions containing 0.33 mM Co(II) in 50 mM Tris/Cl^- buffer. This is about half the amount of phenol required to saturate the human insulin hexamer under the same conditions. In the absence of phenol, the spectra are characteristic for octahedral Co(II) complexes, with an increased baseline at pH 7.1. The higher baseline is presumably due to increased scattering by high molecular weight aggregates. Nevertheless, with a phenol concentration of 5 mM, an appreciable absorbance from tetrahedral Co(II) is observed at both pH 7.1 and 8.0.

DISCUSSION

Ligand Binding to Co(II)-Human Insulin

The phenolic ligand binding and extraction profiles presented in Figure 1 clearly establish the order of ligand binding affinities to the insulin hexamer as resorcinol >> phenol > m-cresol. It is also apparent that the different affinities are more easily observed in the extraction experiments when compared to formation experiments. In general, the formation rates are not significantly different between either phenolic ligands or the two trimers. The overall similarity between these formation rates is not surprising considering the ligands do not differ significantly in their size and structure. The increase in the binding rates for m-cresol is attributed to it being more hydrophobic relative to phenol and resorcinol; therefore, it binds more quickly to the hydrophobic binding pockets in the hexamer. Once m-cresol binds, the energetics for it to remain liganded must be less favorable as evidenced by the increasing absorbance of tetrahedral Co(II) centers between m-cresol, phenol, and resorcinol binding; i.e., the equilibrium constant for the $T_6 \leftrightarrow T_3R_3$ transition (k_1/k_{-1} in eqn. 2) is smallest for m-cresol binding despite the larger value of k_1.

The biphasic nature of the kinetic profiles and amplitude convergence to 0.5 indicates that the Co(II)-insulin system demonstrates substantial negative inter-trimer cooperativity with the T_3R_3 hexamer as an intermediate. This is in agreement with previous observations cited in the literature (7–9). The strong nonlinear dependence of the observed rates on phenolic ligand concentration for both phases and all ligands (Figure 2, Table I) was expected from the model (eqns. 5 and 6). Two results of the negative cooperative binding and subsequent biphasic kinetics are: (1) the greater ligand concentration dependency in the second trimer relative to the first trimer and (2) a difference in the off rates, k_{-1} and k_{-2}, where the former must be of lower magnitude due to the equivalence of k_1 and k_2.

As mentioned previously, the biphasic nature of the kinetics is due to the substantial negative inter-trimer cooperativity. Charge repulsion created by the close proximity of the six carboxylate groups of the Glu^{B13} residues in the R_6 hexamer is believed to cause the negative inter-trimer cooperative effect (23–25). If formation of the second R_3 trimer is inhibited by charge repulsion created by the Glu^{B13} residues, then a slower rate of formation is expected because of the difficulty in converting the trimer monomers to the R-state to allow subsequent binding of phenolic ligands (Figure 1A). This will also decrease the intra-trimer cooperative binding in the second trimer relative to the first.

With both trimers, the less than cubic dependence on the observed rate with ligand concentration may indicate either the presence of inter- and intra-trimer cooperativity or a competing mechanistic step of similar rate (e.g., the formation of the ligand-binding pocket or another intermediate that may slow this phase of the reaction). The increased power dependence on the ligand concentration for intra-trimer binding in the slow phase can be attributed, in part, to the negative inter-trimer

cooperativity making the binding to the second trimer more difficult. A decrease in the intra-trimer cooperative binding may also serve to increase the ligand concentration power dependence. This is consistent with equilibrium binding studies, which display prolonged concentration dependence for the binding in the second phase of the profiles (15).

The kinetics of m-cresol binding to Co(II)-insulin hexamers was studied previously (12). The authors stated that m-cresol binding to insulin hexamers was biphasic with a concentration-dependent fast phase and a concentration-independent slow phase. Upon careful inspection of our data, we can only conclude that observed rates in both phases are highly ligand-concentration dependent for all phenolic ligands studied. The concentration dependence of the ligand binding rates was expected because the probability of the molecular event required to produce a reaction (i.e., m-cresol binding to T_3R_3 insulin hexamer) increases with the concentration of the reactants.

Extraction of Co(II) from R_6 Human Insulin Hexamers

Once the R_6 hexamer is formed with six phenolic ligands bound, extraction of the metal ion is more readily influenced by the affinity of the bound ligand. Because access to the metal ion is highly restricted by the compact structure of the insulin hexamer, and the kinetics of the reaction is slow, we assume that extraction occurs via a T-state hexamer (T_6, T_3R_3, or suitable intermediate) and that k_{-2} in equations 3 and 7 is rate limiting. Therefore, differences in ligand binding affinities are more easily observed with metal ion extraction experiments.

The ligand with the greatest affinity for the insulin hexamer, resorcinol, binds more tightly because of additional hydrogen bonds formed through its second hydroxyl group. X-ray crystallography has shown that resorcinol binds to the Zn(II) insulin hexamer in a similar manner as phenol, but in addition there is a strong hydrogen bond between the second hydroxyl group and the carbonyl group of the Cys^{A11} on the same insulin monomer via a bridging water molecule as well as a possible, albeit weak, hydrogen bond interaction to an imidazole nitrogen of a His^{B5} on an adjacent insulin monomer (G. D. Smith, personal communication). Because additional energy will be required to break the extra hydrogen bond(s), the rate constant for the $R_6 \rightarrow T_3R_3$ transition (k_{-2}, equation 6) is significantly less with resorcinol. The increase in the extraction rate when m-cresol is the binding ligand may be attributed to steric hindrance from the methyl group, which causes less favorable contacts relative to phenol and resorcinol (Figure 1B).

With k_{-2} being rate limiting, the apparent zero-order dependence of the rate on EDTA concentration is due to either saturating levels of chelator relative to the concentration of T-state hexamers from which extraction occurs or that the extraction step is fast compared to previous steps. This is true even if just enough EDTA is added to match the Co(II) 1:1 stoichiometrically. If the insulin solution is not saturated with phenolic ligand and therefore a significant population of T_3R_3 hexamers is present, a linear dependence of the extraction rate on EDTA concentration is observed. Coupled with the inverse linear dependence on chloride concentration (data not shown), these results are consistent with the proposed mechanism.

The $T_3R_3 \leftrightarrow R_6$ Equilibrium Constant in the Co(II)/Human Insulin System

The equilibrium constant for the $T_3R_3 \leftrightarrow R_6$ transition (Table I) is calculated using the rate constants, k_2 and k_{-2} (eqn. 3) determined from formation and extraction experiments, respectively. For comparison, the equilibrium constants obtained for the $T_3R_3 \leftrightarrow R_6$ transition from modeling binding profiles measured by isothermal titration calorimetry (26,27) are also given. Considering the differences in the methods used for obtaining this equilibrium constant, the complexity of the phenolic ligand/Co(II)-insulin system, and the magnitude of the number, the agreement is quite reasonable. Although the agreement in these numbers does not necessarily support the argument that extraction occurs via a T_3R_3 intermediate, it does reinforce our hypothesis that extraction does not occur directly from the R_6 hexamer. A slow transition to another intermediate species must occur before extraction takes place. The zero-order dependence on [EDTA] (data not shown) also supports this conclusion.

Phenolic Ligand Binding to Co(II)-LysPro Insulin

The same order of ligand binding affinities exists with the LysPro hexamer as with human insulin (i.e., resorcinol >> phenol > m-cresol). However, relative to human insulin, the binding of phenolic ligands to LysPro insulin solutions that contain Co(II) is more complex. In considering all of the available data, we offer the following plausible interpretation of the pH dependent kinetic results. The model presumes that a hexameric complex must be established prior to phenolic ligand binding.

pH 8.0

At pH 8.0, two ligand concentration-independent kinetic phases are observed. As a result of the poorly defined association state of LysPro insulin, our interpretation of the binding kinetics is severely limited. Thus, the following mechanism is proposed:

$$A \underset{\rightarrow}{\overset{k^d}{\leftarrow}} X_{(i<6)} \tag{12}$$

$$X_{(i<6)} + Co(II) \underset{\rightarrow}{\overset{k^a}{\leftarrow}} H + \phi \underset{\leftarrow}{\overset{k^\phi}{\rightarrow}} R_6 \tag{13}$$

where, at pH 8.0, "*A*" refers to low molecular weight Co(II)-LysPro aggregates with sedimentation coefficients centered at $S = 3.8$ as observed by ultracentrifugation (Table III), k_d is the dissociation rate of these aggregates, and i represents the number of LysPro monomers. The rate of association of Co(II) and LysPro monomers (or species with $S < 3.80$) to the hexamer species (H) that binds phenolic ligand (ϕ) is given by k_a. The rate of phenolic ligand binding is k_ϕ.

It is presumed that the slow phase ($\overline{k_{slow}}$, Table II) observed in the binding kinetics is the dissociation of the aggregates represented in equation 12. The faster, ligand-concentration-independent phase ($\overline{k_{fast}}$, Table II), is the association of $X_{i<6}$ into hexameric complexes that can bind phenolic ligands (eqn. 13). The two phases are observed because both aggregate

and $X_{i<6}$ are present prior to the addition of phenolic ligands. The existence of aggregate and $X_{i<6}$ species is consistent with the polydisperse pattern observed in the sedimentation velocity experiments. Thus, the observed ligand-concentration-independent kinetics at pH 8.0 support our minimal mechanism if the relative order of rate constants is then $k_\phi > k_a > k_d$. It should be stressed that hidden processes not detectable by our experimental method are possible, and even seem likely from such a disordered system. Thus, the two phases resolved in our experimental analysis likely represent a composite of multiphasic processes.

pH 8.0 (pre-treated)

In order to begin from a more well-defined state, the kinetics of phenolic ligand binding to LysPro hexamers in the presence of Co(II) was measured with the protein solution pre-treated to sub-saturating concentrations of ligand. The addition of a relatively small amount of phenolic ligand drives a majority of the LysPro into a hexameric state (Table III). The relative amount of liganded sites is 40% to 60% of the saturating value for phenol and resorcinol, respectively. The decrease in the sedimentation coefficient and the polydispersity (Table III) clearly shows that the aggregate present in the untreated solution has been eliminated, and that a significant population of LysPro hexamer now exists in equilibrium with a smaller population of lower molecular weight species, i.e., monomers, dimer, etc. The ligand-binding kinetics displayed in Figure 3 would then suggest that the ligand-concentration-dependent fast phase (k, Table I) is a result of ligand binding to a pre-established hexameric intermediate, which is then driven to the R_6 complex (eqn. 14)

$$H_{(\phi<6)} + \phi \underset{\leftarrow}{\overset{k^{\phi'}}{\rightarrow}} R_6 \qquad (14)$$

where $H_{(\phi<6)}$ is a partially liganded Co(II)-LysPro hexamer. The slow-ligand-concentration independent phase ($\overline{k_{slow}}$, Table II) is described by equation 13. Thus, for this minimal mechanism to conform to the observed kinetics, the limiting rates for the fast and slow phases are k'_ϕ and k_a, respectively. The observed rates of ligand binding for the concentration-dependent phase are comparable to but faster than that of human insulin. This may be attributed to more accessible binding sites on an expanded LysPro hexamer relative to human insulin. The significantly decreased amplitude in the slow ligand-concentration-independent phase is due to the domination of the $H_{(\phi<6)}$ species in the pre-treated solution.

The intermediate(s) has/have not been defined, but is/are assumed to be a combination of several different hexamer species with varying degrees of saturation, including T_3R_3. Inter-trimer cooperativity is less of a factor in LysPro insulin (>95% of the binding sites are saturated at ≈20 mM relative to 40 mM for human insulin). Therefore, liganded hexameric species other than T_3R_3 are expected to contribute to the binding kinetics in the pre-treated solution.

In the pre-treated solution, the observed rate for the ligand-concentration-independent slow phase ($\overline{k_{slow}}$, Table II) remains unchanged from the untreated data (Table II) and is consistent with assignment as k_a in equation 13. However, the amplitude of the slow phase has decreased significantly (approximately 30%). The presence of this concentration-independent-phase and the non-symmetrical profiles observed in the sedimentation velocity experiments indicate that species with molecular weights less than that of a hexamer still exist. Thus, in order to explain the observed ligand-concentration-independent and -dependent rates, the relative order of rates is then $k'_\phi > k_\phi > k_a$. The two kinetic phases are the result of $H_{(\phi<6)}$ and $X_{(i<6)}$ species that are initially present in the pre-treated solution.

pH 7.1

At pH 7.1 the binding of phenolic ligands to Co(II)-LysPro is also biphasic, with ligand-concentration-dependent fast, and -independent slow phases. The same mechanism described in equations 12 and 13 can be used here with the substitution of high molecular weight aggregates for A, and with k_d as the rate-determining constant for the slow phase. The considerably higher molecular weights observed for the Co(II)-LysPro complex at pH 7.1 are believed to be due to the decreased negative charge on the monomers, which subsequently decreases the intermolecular repulsive forces and allows for greater association. In order to explain the observed ligand concentration dependence, k_ϕ must be rate determining in equation 13 rather than the pH dependent k_a. Therefore, the relative rates of binding are $k_a > k_\phi > k_d$.

The comparable observed fast rate for Co(II)-LysPro relative to the fast rate observed in Co(II)-human insulin (magnitude of y-axes in Figures 2A and 4A) is interesting but probably coincidental. It seems unlikely that the fast phase in LysPro at pH 7.1 is due to the $T_6 \rightarrow T_3R_3$ transition considering the polydisperse nature of the protein prior to the addition of ligand. Also, a large discrepancy exists between n^{th}-order rate constants and ligand-concentration-power dependence in the fast phase for human and LysPro insulin (Table I). The spectroscopic fingerprint of the ligand-bound complex is that of a tetrahedral Co(II)-insulin complex; therefore, the fast phase is due to binding phenol to Co(II)-LysPro hexamers. Coupled with the reduced ligand concentration required for saturation (about half relative to human insulin), the Co(II)-LysPro species monitored with the fast phase at pH 7.1 is probably a mixture of liganded hexamer intermediates all contributing to the measured absorbance of tetrahedral Co(II) centers.

The increased rate of binding and the power dependence associated with the ligand-concentration-dependent phase are consistent with less intra- and inter-trimer cooperativity in the Co(II)-LysPro hexameric system.

Cooperativity

In the Co(II)-insulin hexamer, phenolic ligand binding is modulated by positive intra-trimer and substantial negative inter-trimer cooperativity (9). In Co(II)-LysPro hexamers, it appears that both intra- and inter-trimer cooperativity are reduced as evidenced by the lower ligand concentration required for saturation of the hexamer, the inability to see more than one ligand concentration dependent binding phase, and the increased power dependence (relative to insulin) in the modeling of the kinetic binding data. All of these results suggest a hexamer that demonstrates decreased cooperative binding relative to human insulin that may be due, in part, to structural

changes associated with the sequence inversion observed in the hexameric complex (6).

Extraction of Co(II)-from R_6 LysPro Insulin Hexamers

The slow extraction rate observed with LysPro hexamers suggests this analog adopts a R_6-type structure in solution and restricts the access to the metal ion. This structure is not unexpected since X-ray crystallographic data has revealed the presence of a LysPro $T_3R_3^f$ (6) and an apparent R_6-type hexamer (16). These crystal structures show a highly restricted metal site in the R_3^f trimer located at the bottom of an approximately 20 Å channel. In these extraction experiments, the LysPro hexamer is initially saturated with ligand; therefore, the starting point is that of discrete R_6-type hexamers. Extraction from the R_6-type LysPro hexamer is very similar to that of human insulin with respect to the monophasic profiles, the rate of the reaction, and chloride and EDTA concentration dependencies. Modeling the extraction kinetics in the same way as that of insulin yields similar values for the rate limiting k_{-2}. More importantly, the value of k_{-2} is independent of pH with LysPro, suggesting that the rate-limiting process that controls metal ion extraction is an intramolecular property of the LysPro hexamer. Therefore, the initial phase of the reaction appears to be very similar to the process that occurs in human insulin. However, once past the rate-limiting phase of the reaction, the extraction kinetics are affected by intermolecular properties such as association of LysPro insulin. Therefore, the factor k in equation 8 may differ significantly between insulin analogs, as demonstrated by calculating the apparent equilibrium constants from modeling the extraction kinetics. The values for $K_{kinetic}$ in Table I are obtained from fitting the ligand-concentration-dependent extraction data with equation 11. The difference in $K_{kinetic}$ between insulin and LysPro at pH 8.0 (four orders of magnitude) is largely attributed to differences in k.

Conclusions and Physiological Implications

With LysPro insulin, the kinetics of phenolic ligand binding and metal ion extraction, along with equilibrium visible absorption and ultracentrifugation data, strongly suggest the presence of R_6-type hexamers in solution at saturating levels of phenolic ligand. However, the path taken to form these R_6 hexamers is quite different from that of human insulin, initiating with the protein in a polydisperse, highly aggregated state and proceeding to a discrete R_6 complex. The existence of discrete hexamer intermediates such as T_6 and T_3R_3 cannot be determined from this data. However, an X-ray crystal structure of a $T_3R_3^f$ hexamer suggests that intermediates similar to that of human insulin can exist in solution. Further evidence that supports intermediates such as $T_yR_{(6-y)}$ is the ligand-concentration-dependent rates observed in the binding kinetic data generated for ligand-treated LysPro solutions at pH 8.0 and the ligand concentration-dependent phase for LysPro solutions at pH 7.1.

The disruption kinetics at or near neutral pH provides evidence of a R_6 complex that has a significantly different dissociation process for the LysPro hexameric complex ($k_{LysPro} >> k_{insulin}$). The drastically different kinetics measured for LysPro hexamers relative to insulin hexamers demonstrates that equilibrium binding data would be insufficient in the determination of mechanisms of association and dissociation. Therefore, the kinetic analysis is necessary because it effectively highlights the differences between the two insulin species.

The inability of LysPro to form discrete T_6-hexamer complexes and the radically different dissociation process both support a pathway that can potentially lead directly to a monomeric species. Our results comparing human and LysPro insulin provide further insight into the mechanisms of assembly and dissociation governing the differences in physiological properties. These results are consistent with a pharmacokinetic model reported by Ciszak *et al.* (6) that requires diffusion of the phenolic ligand; however, our results suggest that diffusion of the metal ion from the site of subcutaneous injection is also necessary to avoid any higher-order, non-native association from occurring, which could hinder absorption.

ACKNOWLEDGMENTS

The authors wish to thank Allen Pekar for help in obtaining the ultracentrifugation data, as well as Mark Brader, Bruce Frank, Alex Glazer, Henry Havel, and Maryanne Wagner for critical review of the manuscript.

REFERENCES

1. J. Brange and L. Langkjaer. *Acta Pharm. Nord.* **4**:149–158 (1992).
2. U. Derewenda, Z. Derewenda, E. J. Dodson, G. G. Dodson, C. D. Reynolds, G. D. Smith, C. Sparks, and D. Swenson. *Nature* **338**:594–596 (1989).
3. A. Wollmer, B. Rannefeld, B. R. Johansen, K. R. Hejnaes, P. Baldschmidt, and F. B. Hansen. *Biol. Chem. Hoppe-Seyler* **368**:903–911 (1987).
4. G. D. Smith and E. Ciszak. *P.N.A.S.* **91**:8851–8855 (1994).
5. E. N. Baker, T. L. Blundell, J. F. Cutfield, S. M. Cutfield, E. J. Dodson, G. G. Dodson, D. M. C. Hodgkin, R. E. Hubbard, N. W. Isaacs, C. D. Reynolds, K. Sakabe, N. Sakabe, and N. M. Vijayan. *Phil. Trans. R. Soc. Lond. B* **319**:369–456 (1988).
6. E. Ciszak, J. M. Beals, B. H. Frank, J. C. Baker, N. D. Carter, and G. D. Smith. *Structure* **3**:615–622 (1995).
7. M. L. Brader and M. F. Dunn. *TIBS* **16**:341–345 (1991).
8. M. Roy, M. L. Brader, R. W.-K. Lee, N. C. Kaarsholm, J. F. Hansen, and M. F. Dunn. *J. Biol. Chem.* **264**:19081–19085 (1989).
9. P. Krüger, G. Gilge, Y. Çabuk, and A. Wollmer. *Biol. Chem. Hoppe-Seyler* **371**:669–673 (1990).
10. N. C. Kaarsholm, H.-C. Ko, and M. F. Dunn. *Biochemistry* **28**:4427–4435 (1989).
11. N. C. Kaarsholm and M. F. Dunn. *Biochemistry* **26**:883–890 (1987).
12. Y. Karatas, P. Krüger, and A. Wollmer. *Biol. Chem. Hoppe-Seyler* **372**:1035–1038 (1991).
13. M. C. Storm and M. F. Dunn. *Biochemistry* **24**:1749–1756 (1985).
14. D. N. Brems, L. A. Alter, M. J. Beckage, R. E. Chance, R. D. DiMarchi, L. K. Green, H. B. Long, A. H. Pekar, J. E. Shields, and B. H. Frank. *Protein Engineering* **5**:527–533 (1992).
15. D. L. Bakaysa, J. Radziuk, H. A. Havel, M. L. Brader, S. L. Edwards, S. W. Dodd, J. M. Beals, A. H. Pekar, and D. N. Brems. Physiochemical basis for the rapid time-action of $Lys^{B28}Pro^{B29}$-Insulin: Dissociation of a protein ligand complex. *Protein Sci.: in press.*
16. E. Ciszak, D. Langs, J. M. Beals, B. H. Frank, and G. D. Smith. *A novel crystal form of LysPro insulin.* In *American Crystallographic Association Annual Meeting*, Montreal, American Crystallographic Association, 1995.
17. D. C. Howey, R. R. Bowsher, R. L. Brunelle, and J. R. Woodworth. *Diabetes* **43**:396–402 (1994).
18. J. Brange, D. R. Owens, S. Kang, and A. Volund. *Diabetes Care* **13**:923–954 (1990).
19. B. H. Frank and A. J. Veros. *Biochem. Biophys. Res. Com.* **32**:155–160 (1968).
20. K. E. van Holde. Physical Biochemistry. Prentice-Hall, Inc., Englewood Cliffs, NJ, 1985, pp. 110–136.

21. L. Gross and M. F. Dunn. *Biochemistry* **31**:1295–1301 (1992).
22. P. Brzovic S., W. E. Choi, D. Borchardt, N. C. Kaarsholm, and M. F. Dunn. *Biochemistry* **33**:13057–13069 (1994).
23. A. Wollmer, B. Rannefeld, J. Stahl, and S. G. Melberg. *Biol. Chem. Hoppe-Seyler* **370**:1045–1053 (1989).
24. E. Jacoby, P. Kruger, Y. Karatas, and A. Wollmer. *Biol. Chem. Hoppe-Seyler* **374**:877–885 (1993).
25. C. R. Bloom, W. E. Choi, P. S. Brzovic, J. J. Ha, S. T. Huang, N. C. Kaarsholm, and M. F. Dunn. *J. Mol. Biol.* **245**:324–330 (1995).
26. A. D. Varshavsky, J. M. Beals, D. T. Birnbaum, S. W. Dodd, and B. E. Saxberg. A combined optimization strategy in mathematical modeling of phenolic ligand binding to the insulin hexamer. *Math. Modeling and Sci. Computing: in press.*
27. D. T. Birnbaum, S. W. Dodd, B. E. H. Saxberg, A. D. Varshavsky, and J. M. Beals. *Biochemistry* **35**:5366–5378 (1996).